Fast response dual-frequency liquid crystal switch with photo-patterned alignments

Xiao-Wen Lin,[1] Wei Hu,[1,4] Xi-Kui Hu,[1] Xiao Liang,[2] Ye Chen,[1] Hong-Qing Cui,[1] Ge Zhu,[1] Jia-Nan Li,[1] Vladimir Chigrinov,[3] and Yan-Qing Lu[1,5]

[1]*National Laboratory of Solid State Microstructures and College of Engineering and Applied Sciences, Nanjing University, Nanjing 210093, China*

[2]*Department of Chemistry, Tsinghua University, Beijing 100084, China*

[3]*Center for Display Research, Department of Electronic and Computer Engineering, Hong Kong University of Science and Technology, Clear Water Bay, Kowloon, Hong Kong, China*

[4]*e-mail: huwei@nju.edu.cn*

[5]*e-mail: yqlu@nju.edu.cn*

Received July 2, 2012; accepted July 19, 2012;
posted July 24, 2012 (Doc. ID 171589); published August 27, 2012

A dual-frequency liquid crystal based optical switch with orthogonally photo-patterned alignments is designed and fabricated. The cell gap is theoretically optimized for high switching performance. The measured extinction ratio of first diffraction order is over 20 dB with a low electric field of 3 V/μm. The switch On-Off time are measured to be 350 µs and 600 µs, respectively, both of which have reached submillisecond scale. Moreover, the switch is polarization independent, which has been predicted theoretically and further proved experimentally. This design is suitable in wide applications requiring fast response and polarizer free properties.

OCIS codes: 160.3710, 050.1950.

Extensive attention has been attracted to tunable passive components such as filters, switches, and modulators. Liquid crystals (LCs) are good candidates for the tuning materials due to their broadband birefringence and continuous tunability by external fields. Response/switching time is a key parameter that determines the performance of these components. For common nematic LCs, it is usually limited to the level of tens of milliseconds. For fast tuning purpose, several approaches have been raised to shorten the response time, including the developments of special materials like blue phase LCs [1,2], cholesteric LCs [3], and ferroelectric LCs [4], as well as specific ways of creating small domains by polymer dispersion [5] or polymer networks [6]. However, the operation voltage is commonly quite high.

Another type of LC materials that suits for fast tuning is dual-frequency liquid crystal (DFLC) [7], which exhibits a positive dielectric anisotropy ($\Delta\varepsilon = \varepsilon_{\parallel} - \varepsilon_{\perp} > 0$) when frequency f of applied field is below f_c (crossover frequency) while turns to a negative one ($\Delta\varepsilon < 0$) at $f > f_c$. This property enables the possibility of tuning LC orientations by dual-frequency addressing at a relatively low voltage, permitting a fast switching time down to submilliseconds [8,9]. Dual-frequency liquid crystal devices such as optical retarder [10] and variable optical attenuator [11] have been reported with response time ~0.5 ms at $V_{\mathrm{rms}} = 25$ V and ~0.9 ms at $V_{\mathrm{rms}} = 20$ V, respectively.

In DFLC devices, hybrid aligned nematic (HAN) structure with one substrate homeotropically aligned (VA) and the other homogeneously aligned (PA) is often used. The hybrid aligned nematic cell is known to have no Freedericks transition threshold, but only half of LC refractive index change could be utilized. The combination of DFLC and HAN structure could overcome this drawback. However, similar as in most other nematic LC devices, polarization dependency is still a limitation for certain applications. One solution is to create microstructures in LC alignments either by the rubbing method [12] or photoalignment technique [13,14]. The latter has attracted intensive interests for it facilitates pattern fabrication with multi-LC alignments and avoids the problems of the rubbing method, such as contamination, electrostatic charges, and mechanical damage.

Herein, we present a design of forming a patterned DFLC HAN cell [schematically illustrated in Fig. 1(a)] with one substrate having orthogonal PA alignments by a two-step photoaligning, while the other one stayed uniformly VA. This design provides a tunable phase grating, based on which an optical switch is accomplished by controlling the intensity variance of certain diffraction order. The polarization independency of this switch is theoretically proved. Moreover, we optimized the cell gap for better performance. Then the switch is demonstrated according to the optimization and its electro-optical properties are measured.

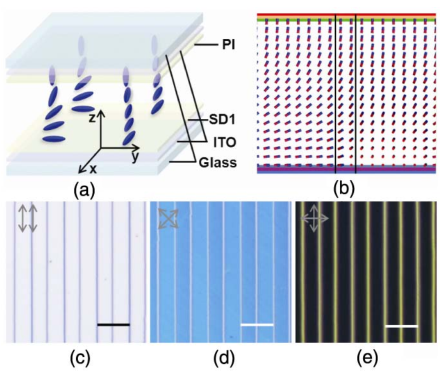

Fig. 1. (Color online) (a) Schematic illustration of the patterned HAN cell; (b) LC director distribution in y-z plane simulated by Techwiz LCD with two black lines marking the boundary region, and (c)–(e) micrographs of the sample, in each of which the relative directions of two polarizers compared with the stripes are labeled in arrows. All scale bars are 20 μm.

0146-9592/12/173627-03$15.00/0

In this patterned HAN cell, the initial elastic director tilt angle could be obtained as $\theta_0(z) = \pi z/2d$, which is approximately a linear function of the LC layer depth z, assuming the cell gap d is along z axis. When an external field E is applied, the director reorients [15]:

$$\theta(z) = \theta_0(z) - \frac{\Delta\varepsilon E^2}{2k}\left(\frac{d}{\pi}\right)^2 \sin\left(\frac{\pi z}{d}\right). \quad (1)$$

The effective refractive index n_{eff} of each region is determined by $\theta(z)$:

$$n_{\text{eff}}(z) = \frac{n_e n_o}{\sqrt{n_e^2 \sin^2\theta(z) + n_o^2 \cos^2\theta(z)}}. \quad (2)$$

When a monochromatic light beam of wavelength λ is incident onto the cell, it could be decomposed into two components, polarized along the two alignment directions [defined as x and y-axis shown in Fig. 1(a)]. The two components experience individually a refractive index change (Δn_x or Δn_y) between two adjacent regions, thus induces phase retardation defined as $\Delta\varphi_x$ or $\Delta\varphi_y$, respectively. As Δn_x and Δn_y have the same absolute value of $\Delta n_{\text{eff}} = n_{\text{eff}} - n_o$, then $\Delta\varphi_x$ and $\Delta\varphi_y$ could be calculated as:

$$|\Delta\varphi_x| = |\Delta\varphi_y| = \int_0^d \frac{2\pi}{\lambda}(n_{\text{eff}}(z) - n_o)\mathrm{d}z = \Delta\varphi. \quad (3)$$

The diffraction efficiencies in x and y directions of nth order ($\eta_{x,n}$ and $\eta_{x,n}$) can be expressed as [16]:

$$\eta_{x,n} = \eta_{y,n} = \frac{1}{n^2\pi^2}(1 - \cos\Delta\varphi)\left(1 - \cos\frac{2\pi n l}{\Lambda}\right) = \eta_n, \quad (4)$$

where Λ represents the period of the gratings while l means the width of one region. Thus, the intensity of nth diffraction order I_n can be written as:

$$I_n = \eta_n E^2(\cos^2\alpha + \sin^2\alpha) = \eta_n E^2, \quad (5)$$

α is the angle between incident polarization and x-axis.

Thus, we have theoretically proved the polarization independency of the proposed switch.

The LC molecules tend to realign along the direction of electric field at $f < f_c$; thus, when applied voltage reaches saturation, the cell would be uniformly VA, i.e., only the zeroth order remains. This is the Off state for the first order. On the contrary, at $f > f_c$, the cell would exhibit alternating orthogonal PA [16] at saturation voltage, then the phase retardation between two adjacent regions can be simplified as:

$$\Delta\varphi = \frac{2\pi}{\lambda}\Delta n d. \quad (6)$$

The intensity of the first order is dependent on the phase retardation between adjacent regions. In order to realize high switching performance, we hope that the intensity of the first order can reach a maximum at saturation voltage. From Eq. (4), we can see that in order to get a maximal η_1, two conditions need to be satisfied: 1) $\cos(2\pi l/\Lambda) = -1$ and 2) $\cos\Delta\varphi = -1$. The former one holds when $l/\Lambda = 1/2$, i.e., the two adjacent regions are equal in size; while the latter one is satisfied when $\Delta n d = (2m+1)\lambda/2$, where m is an integral. Herein, $\Delta n = 0.191$ and $\lambda = 632.8$ nm, therefore, we can get that $d = 1.66\ \mu$m ($m = 0$), 4.97 μm ($m = 1$), 8.28 μm ($m = 2$), etc. We choose 4.97 μm on balance, considering that large cell gap would lead to the increase of response time as well as operation voltage, while thinner cell would suffer more severe influence due to the inevitable cell gap fluctuation during the experiment.

Then our cell construction is carried out according to the theoretical optimization. To realize the patterned HAN cell design, two ITO-coated glass substrates are coated with different alignment layers separately. For the VA one, a polyimide (PI-5661, Nissan, Japan) layer is used; for the patterned PA, photo-sensitive sulfonic azo-dye (SD1, DIC, Japan) is employed. This substrate is exposed twice under a linearly polarized blue LED to form orthogonal alignments [16]. The two adjacent regions are controlled equal in size by a mask with 10 μm stripes separated by 10 μm spaces, and one of the alignments is along the stripes. The two substrates are then assembled together separated by 5 μm spacers. The measured cell gap is $5.1 \pm 0.1\ \mu$m. The DFLC (HEF951800-100, HCCH, China) is infiltrated into the cell with its physical properties listed as follows: $n_o = 1.498$, $\Delta n = 0.191$ (at $\lambda = 633$ nm and $T = 24\,^\circ$C), $\Delta\varepsilon = 2.10$ at $f = 1$ kHz and -2.02 at $f = 80$ kHz, and $f_c \approx 45$ kHz.

Figures 1(c)–1(e) show the micrographs of the cell observed under a polarizing microscope. Any two adjacent regions are quite uniform in color and brightness except for some boundary lines. The uniformity proves excellent orthogonality of any two adjacent alignments indicating the property of high polarization independency. The occurrence of boundary lines could be explained with the continuum theory, that is, at the boundary of different alignments, a transitional area of LC orientations would be formed because the molecules are influenced by both regions. This causes phase retardation differences that lead to boundary lines in micrographs. Above analysis is further proved through simulations by Techwiz LCD (Sanayi System Co., Korea). Figure 1(b) presents cross-sectional (y-z plane) director distribution of the sample at voltage Off state from which

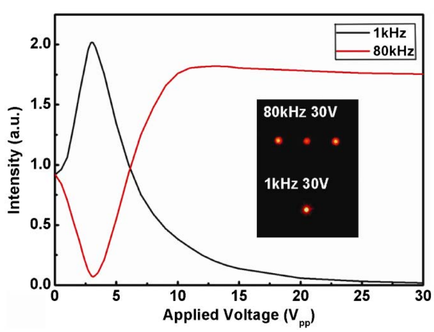

Fig. 2. (Color online) Voltage dependent intensities of first order at 1 kHz and 80 kHz. Insets show diffraction patterns at the On and Off states.

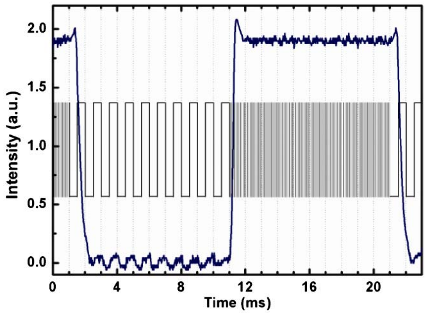

Fig. 3. (Color online) Switch performance of the sample and the applied signals.

we can clearly observe the continuous change of LC orientations at the boundary, as emphasized by two lines.

The electro-optical properties of the proposed switch are tested. Figure 2 exhibits two voltage-intensity curves of first order measured when rectangular electric signals are applied at $f = 1$ and 80 kHz, respectively. At saturation voltage, the intensity is suppressed at 1 kHz while keeping strong at 80 kHz. So the switching effect could be achieved through frequency alternating at a given voltage above saturation. From our analysis, a maximum intensity should be achieved at saturation state at 80 kHz. However, a slightly decline is observed, which means the actual phase retardation is a little more than 3π, our theoretically estimated value (representing the intensity maximum). This is because the cell gap is slightly larger than the optimized result. Yet the extinction ratio exceeds 20 dB, which is already applicable. The insets visually reveal the high switch performance. Further improvement on extinction ratio is achievable by more precise cell gap control and employing a quarter-waveplate that can greatly eliminate the residual phase; thus, reducing the intensity at the Off state [17].

As a key parameter, the switching time is measured. As illustrated in Fig. 3, a 30 V_{pp} signal is utilized with frequency alternating between 1 and 80 kHz, lasting for 10 ms each. Two small protrudes are observed at the On state, standing for the intermediate states of 3π phase retardation during switching. Submillisecond switching has been achieved, with measured On–Off time (defined as the duration time that intensity changes from minimum to maximum and reverse) of 350 μs and 600 μs, respectively. Further improvement could be accomplished by increasing voltages. For instance, the On–Off times reduce to 280 μs and 460 μs, respectively, at 50 V_{pp}.

The polarization independency is demonstrated by rotating the sample. The voltage intensities of first order are presented in Fig. 4, when the sample placing in three different directions: 0, 45, and 90 deg relative to the incident polarization at $f = 1$ and 80 kHz. Curves measured at the same frequency are in high accordance with each other, as predicted in previous analysis.

In summary, we proposed and demonstrated a polarizer free fast response DFLC switch with patterned HAN structures. The cell gap is theoretically optimized for better extinction ratio, the measured value of which is over 20 dB. The switch On-Off time both reach submillisecond scale, 350 μs and 600 μs, respectively, with a low electric field of 3 V/μm. Besides fast switching and polarization independency, advantages such as simple structure, easy fabrication, cost efficiency, and feasibility for mass production make the device competitive.

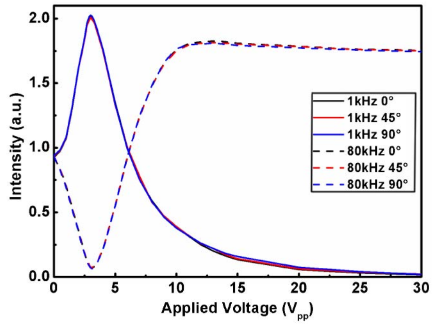

Fig. 4. (Color online) Voltage dependent intensities of first order at 1 kHz and 80 kHz when the sample placing at three different directions: 0, 45, and 90 deg relative to the incident polarization.

This work is sponsored by 973 programs (2011CBA00200 and 2012CB921803), the Hong Kong University of Science and Technology (HKUST) grant (CERG 612310), and the Natural Science Foundation of Jiangsu Province (NSFJP) program (BK2010360). The authors also acknowledge support from the Priority Academic Program Development of Jiangsu Higher Education Institutions (PAPD) and the Fundamental Research Funds for the Central Universities (FRFCU).

References

1. J. Yan, Y. Li, and S. T. Wu, Opt. Lett. **36**, 1404 (2011).
2. G. Zhu, J. N. Li, X. W. Lin, H. F. Wang, W. Hu, Z. G. Zheng, H. Q. Cui, D. Shen, and Y. Q. Lu, J. Soc. Inf. Disp. **20**, 341 (2012).
3. B. I. Senyuk, I. I. Smalyukh, and O. D. Lavrentovich, Opt. Lett. **30**, 349 (2005).
4. A. K. Srivastava, E. P. Pozhidaev, V. G. Chigrinov, and R. Manohar, Appl. Phys. Lett. **99**, 201106 (2011).
5. Y. H. Fan, H. W. Ren, X. Liang, Y. H. Lin, and S. T. Wu, Appl. Phys. Lett. **85**, 2451 (2004).
6. Y. H. Wu, Y. H. Lin, Y. Q. Lu, H. W. Ren, Y. H. Fan, J. R. Wu, and S. T. Wu, Opt. Express **12**, 6377 (2004).
7. H. Q. Xianyu, S. T. Wu, and C. L. Lin, Liq. Cryst. **36**, 717 (2009).
8. P. D. Brimicombe, L. A. Parry-Jones, S. J. Elston, and E. P. Raynes, J. Appl. Phys. **98**, 104104 (2005).
9. Y. Huang, C. H. Wen, and S. T. Wu, Appl. Phys. Lett. **89**, 021103 (2006).
10. A. B. Golovin, S. V. Shiyanovskii, and O. D. Lavrentovich, Appl. Phys. Lett. **83**, 3864 (2003).
11. X. Liang, Y. Q. Lu, Y. H. Wu, F. Du, H. Y. Wang, and S. T. Wu, Jpn. J. Appl. Phys. **44**, 1292 (2005).
12. J. Chen, P. J. Bos, H. Vithana, and D. L. Johnson, Appl. Phys. Lett. **67**, 2588 (1995).
13. V. G. Chigrinov, V. M. Kozenkov, and H. S. Kwok, *Photoalignment of Liquid Crystalline Materials: Physics and Applications* (Wiley, 2008).
14. H. Wu, W. Hu, H. C. Hu, X. W. Lin, G. Zhu, J. W. Choi, V. Chigrinov, and Y. Q. Lu, Opt. Express **20**, 16684 (2012).
15. Y. Q. Lu, X. Liang, Y. H. Wu, F. Du, and S. T. Wu, Appl. Phys. Lett. **85**, 3354 (2004).
16. W. Hu, A. K. Srivastava, X. W. Lin, X. Liang, Z. J. Wu, J. T. Sun, G. Zhu, V. Chigrinov, and Y. Q. Lu, Appl. Phys. Lett. **100**, 111116 (2012).
17. X. J. Wang, Z. D. Huang, J. Feng, X. F. Chen, X. Liang, and Y. Q. Lu, Opt. Express **16**, 13168 (2008).